Acta Astronautica 236 (2025) 627–635

Contents lists available at ScienceDirect

Acta Astronautica

journal homepage: www.elsevier.com/locate/actaastro

Analysis of the mass transport properties of the binary polymeric mixture in microgravity conditions during the DCMIX4 campaign onboard the ISS. Comparison with gravity-based experiments

Antton Sanjuan [a], Daniel Sommermann [b], Werner Köhler [b], Henri Bataller [c], Fabrizio Croccolo [c], Aliaksandr Mialdun [a], Valentina Shevtsova [a,d], M. Mounir Bou-Ali [a,*]

[a] Fluid Mechanics Group, Faculty of Engineering, Mondragon University, Loramendi 4, Apdo. 23, Mondragon, 20500, Spain
[b] Physikalisches Institut, Universität Bayreuth, Bayreuth, 95440, Germany
[c] Universite de Pau et des Pays de l'Adour, E2S UPPA, CNRS, TOTAL, LFCR UMR5150, Anglet, France
[d] IKERBASQUE, Basque Foundation for Science, 48071, Bilbao, Spain

ARTICLE INFO

Keywords:
DCMIX4
Microgravity
Thermodiffusion
Macromolecule

ABSTRACT

We present the results of thermodiffusion experiments conducted under microgravity conditions during the DCMIX4 mission performed onboard the International Space Station (ISS). The space data are compared to previously obtained ground-based measurements. The investigated binary mixture, composed of polystyrene (4730 g/mol) dissolved in the pure solvent toluene, was analysed at four different operating temperatures: 20-25-30-35 °C. A complete procedure was developed, detailing each step from data acquisition to the determination of the fluid transport properties (Soret, molecular diffusion, and thermodiffusion coefficients) using various analytical solutions. Experimental results for the Soret coefficient (steady-state species separation analysis) indicate a linear decrease with increasing temperature, which is in excellent agreement with the Soret coefficients obtained under ground-based thermodiffusion experiments. In contrast, the molecular diffusion coefficient (unsteady-state study) exhibits an increasing trend with temperature, presenting larger deviations from gravity-based results. These variations are attributed to inaccuracies in phase reconstruction because of limitations in the employed phase-stepping technique.

1. Introduction

Transport phenomena encompass the investigation of the exchange of mass, momentum, and energy between different volume elements of a thermodynamic system. In natural processes, it is common for matter in liquid, gas, or solid states to exhibit non-homogeneous distributions, resulting in variations in composition at distinct locations. These compositional differences create disequilibrium, driving the transport of mass, momentum, and energy to try to restore equilibrium. In this context, mass transport can occur through various mechanisms depending on the conditions of the system. Molecular diffusion, for instance, arises in response to concentration gradients in the form of a microscopic random walk of the sample molecules that ends up in fluctuations at any length scales. Alternatively, when mass transport is driven by temperature differences, the phenomenon is referred to as thermodiffusion, which was initially observed by Carl Ludwig and Charles Soret in the 19th century [1]. In this respect, the Soret coefficient (S_T) is the magnitude that relates the thermodiffusion (D_T) and the molecular diffusion (D) coefficients and can exhibit either a positive or negative value [2,3].

In recent years, there has been a significant increase in interest in the study of thermodiffusion and today, this complex phenomenon is not limited to a single application but is fundamental to numerous sectors across a wide range of fields (refer to Refs. [2,3]). In this context, the development and improvement of new applications require prior knowledge of the mass transport properties and therefore, it is essential to investigate the process of species separation in response to temperature gradients in a variety of media [3]. In 1999, with the goal of beginning to acquire this comprehensive understanding, five European laboratories collaborated to systematically analyse and determine the mass transport coefficients of distinct binary liquid mixtures consisting of 1,2,3,4-tetrahydronaphthalene (THN), isobutylbenzene (IBB) and

* Corresponding author.
E-mail address: mbouali@mondragon.edu (M.M. Bou-Ali).

https://doi.org/10.1016/j.actaastro.2025.07.040
Received 20 June 2025; Accepted 18 July 2025
Available online 19 July 2025

n-dodecane (C_{12}), as previously published works showed discrepancies. In this coordinated study, various experimental methodologies were used. Among them, the convective technique of the traditional Thermogravitational Column (TGC) [4] together with the diffusive methods of Thermal Diffusion Forced Rayleigh Scattering (TDFRS) [5] and the Open-Ended Capillary (OEC) [6], were considered. In this way, in 2003, unified transport coefficients were published, today known as the Fontainebleau Benchmark reference systems [7]. To date, these data have served as a reference for the development-validation of new experimental procedures, such as the Optical Beam Deflection (OBD) [8] method and the Optical Digital Interferometry (ODI) [9], applied to a Soret cell, as well as implemented in the thermogravitational microcolumn (μTGC) [10] or the dynamic Shadowgraphy [11], the only optical method that, for binary mixtures, does not reply on the knowledge of optical contrast factors.

In general, the systems involved in natural and industrial processes consist of more than two components. Thus, the next step was to focus on the analysis of ternary systems, being the simplest representation of a multicomponent mixture [12]. However, like what occurred with early studies on binary systems, the mass transport coefficients of ternary mixtures determined by different experimental techniques did not show a good agreement [13,14]. The complexity of analysing ternary mixtures increases, as any convective flow generated by the gravitational effect can interfere with the experiment [15]. Recognising that individual efforts were insufficient, several international groups joined forces to establish a reliable reference dataset for ternary systems. In this context, with the aim of mitigating the potential disturbances caused by gravity in the study of ternary mixtures, the Diffusion Coefficient Measurements in ternary mIXtures (DCMIX) project was launched in order to conduct thermodiffusion experiments under microgravity conditions and complete and corroborate results obtained under ground-based experiments [15–17]. Within the framework of the DCMIX project, four measurement campaigns were carried out on board the International Space Station (ISS) and using the Selectable Optical Diagnostic Instrument (SODI) as experimental technique. In each mission, five ternary systems and a reference binary subsystem were simultaneously studied using a Soret cell array. A brief summary of each conducted campaign is provided below, with emphasis on the research work done to date. The details of the SODI technique are explained in the following section 2.

The first mission, DCMIX1, was completed in January 2012. In this, and as a continuation of the Benchmark Fontainebleau [7], a binary subsystem based on THN|C_{12} was positioned in the reference cell (also called the companion cell) together with the ternary mixture composed of THN|IBB|C_{12} at five different concentrations. Thermodiffusion measurements were conducted at 25 °C, and a first international comparison program was performed in order to evaluate the well-known ternary mixture THN|IBB|C_{12} at a mass fraction of 0.80|0.10|0.10. Thus, today, this ternary system is one of the references for the validation of new experimental approaches [18].

The second campaign, DCMIX2, took place in 2014. The sample cell array contained a binary reference mixture of toluene (Tol) and cyclohexane (Ch), as well as ternary systems including methanol (Meth). Although these mixtures also consist of hydrocarbons, they are significantly more complex than the ones studied in DCMIX1. The binary subsystems of the ternary mixture exhibit negative D_T coefficients over the whole concentration range (Tol|Ch), an immiscibility gap (Meth|Ch) at different mass fractions as well as a sign change in the S_T coefficient (Tol|Meth). In this second mission, it was shown that the Soret separation increases by at least one order of magnitude as it approaches the demixing zone. In addition, thermodiffusion experiments were conducted at different average working temperatures and results revealed a linear dependence of the S_T coefficient in both binary and ternary mixtures [19–21].

The third campaign DCMIX3 of the project shifted focus from hydrocarbon mixtures to analyse for the first time the mass transport properties of aqueous mixtures under microgravity conditions. The binary subsystem was composed of water (H_2O) and ethanol (EtOH), and the five ternary mixtures included the triethylene-glycol (TEG) component. DCMIX3 was originally scheduled for October 2014. However, due to a catastrophic failure during liftoff, experiments were ultimately completed in November 2016. The aqueous system is also characterised by, among other features, the sign reversal of the Soret coefficient in both binary and ternary liquid mixtures. The three binary subsystems have been extensively studied in the literature, with the mass transport properties of the H_2O|EtOH mixture determined through various experimental techniques [8,22–25] In addition, results for the second cell ternary mixture (at 25 °C) obtained both under terrestrial and microgravity conditions were published in Refs. [15,26,27].

The fourth mission DCMIX4 was the last microgravity campaign of the project. To maximise the impact of this flight, various liquid mixtures were delivered to the space station in November 2018. The first three cells were filled with Tol|Meth|Ch components, previously studied in DCMIX2, but at distinct concentrations. The sample in the fourth cell included a ternary system based on fullerene (C_{60}), specifically C_{60}|THN|Tol, marking the first investigation of a complex mixture involving nanoparticles. Additionally, in the companion cell and in the fifth cell macromolecule-based mixtures were positioned composed of polystyrene (Ps) in the pure solvents toluene and cyclohexane. In November 2020, once the data were downloaded from the ISS, the results related to the data quality assessment evaluation were published [28]. The contrast of the images, the saturation, the phase-stepping method quality and the temperature stability recorded during the thermodiffusion experiments were investigated. In parallel, recent works have been published in relation to the determination of the mass transport coefficients of the DCMIX4 mixtures under ground-based thermodiffusion experiments and considering different working conditions, that is temperature and concentration. Specifically, binary nanofluids consisting of C_{60}|THN and C_{60}|Tol [29] as well as subsystems composed of Ps|Tol and Ps|Ch [30] along with the macromolecular ternary system Ps|Tol|Ch [31] have been studied in detail considering various experimental techniques. Experimental studies related to the stability of the binary Tol|Ch have also been performed under ground conditions [32].

As a next step, the determination of the Soret, molecular diffusion and thermodiffusion coefficients of the mixtures delivered in DCMIX4 has been initiated. As a continuation of the recently published work in which the mass transport coefficients of the binary polymeric mixtures were determined and corroborated via the TGC, μTGC, OBD and TDFRS techniques (refer to Ref. [30] for a detailed description), the motivation of the present study has been to initiate the analysis of the microgravity experiments performed on the reference mixture composed of Ps|Tol (Ps molar mass 4730 g/mol and 0.02|0.98 mass fraction) at different operating temperatures: 20-25-30-35 °C, an analysis that is essential for the future investigation of the ternary macromolecular mixture. For this purpose, this work first details the key aspects of the SODI instrument. Next, the complete step-by-step followed pipeline for the determination of the mass transport coefficients is presented. Thus, a first comparison between results obtained in both terrestrial and microgravity conditions for the reference polymeric mixture is provided. In this context, the work has been done in collaboration with three international research groups: Mondragon University (MGEP, Spain), Universität Bayreuth (UB, Germany) and Université de Pau et des Pays de l'Adour (UPPA, France).

2. Experimental technique

The following section describes the SODI experimental technique: design, optical installation and DCMIX experiments procedure. SODI is a removable setup that has been in orbit since 2009. It enables the analysis of refractive index variations in binary and ternary systems via interferometry with the possibility of applying to the sample a temperature gradient. In this context, the instrument comprises two primary components [33]. On the one hand, a Soret cell array accommodates six different mixtures: five ternary systems and one binary reference

sample. The core of each cell is built from a quartz frame that contains a cavity measuring 10 × 10 mm^2 in cross-section. At the same time, this frame is positioned between two nickel-plated copper blocks, which are joined by titanium spacers to maintain a uniform distance and prevent excessive pressure on the quartz frame. The distance between the copper blocks is 5 mm, yielding a sample volume of 0.5 ml (5 × 10 × 10 mm^3) for each cell. As for the filling process, the liquid is injected through an opening in the upper block where a compensation volume is reserved to equilibrate any pressure change. A flexible membrane, which enables this compensation, seals the assembly. Additionally, two independent Peltier elements (positioned at the external side of each copper block, top and bottom) and controlled by proportional-integral-derivative (PID) regulation systems are employed to apply the desired temperature difference to two opposite sides of the sample. Likewise, the operating temperatures are measured using thermistors inserted into openings of the copper blocks (refer to Ref. [33] for a schematic illustration).

On the other hand, SODI contains two independent optical setups called 'bridges', one fixed and the other movable, within which the cell array is positioned (see Fig. 1). For the analysis of the reference binary subsystem, a single-laser interferometer operating at 670.0 nm (Hitachi 6714G), designated as Fixed Red (FR), is installed in the fixed bridge. In contrast, to study the remaining ternary mixtures, a Mach-Zehnder interferometer equipped with two lasers, operating at 670.0 nm (Hitachi 6714G) and 935.0 nm (Nanoplus DFB), is positioned in the movable bridge. The latter is mounted on a rail, allowing it to travel from cell to cell. In this case, the two lasers are referred to as Moving Red (MR) and Moving Near-Infrared (MN), respectively. Each interferometer contains all essential optical components such as mirrors, beam splitters and a CCD camera (DALSA Pantera SA 2M30) with a resolution of 1920 × 1080 pixels. In this context, the optical elements are arranged between the illumination and acquisition blocks. Thus, the lasers emit a light beam from the illumination block, that is separated in two beams with one beam passing through the Soret cell containing the sample while the other one serving as a reference beam. In the acquisition block, the two beams are combined, generating an interference pattern that is subsequently captured using the CCD camera (a schematic illustration is provided in Ref. [33]). In the image acquisition process SODI is based on the phase-shifting technique by introducing phase variations across five consecutively captured images with a maximum delay of 1 s between the acquisition of the first and last image, grouped in what has been called a "stack" of images. Adjustments to the current of the laser source result in changes in the laser wavelength, thereby inducing a phase shift of π/2 between successive images in a stack [28].

Regarding the experimental procedure, three main steps are identified for each thermodiffusion experiment, being the same for both the binary reference subsystem and the ternary mixtures. The first stage involves unmonitored thermal homogenisation, during which the mixture's temperature is stabilised at the mean working temperature

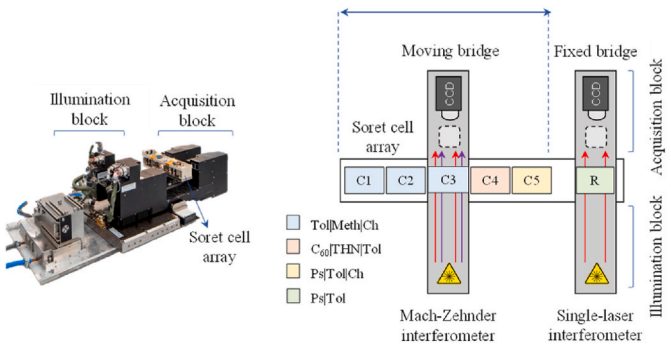

Fig. 1. Experimental apparatus. Picture of the SODI instrument obtained from QuinetiQ Group together with a schematic illustration created for DCMIX4: the Soret cell array, the optical bridges and the illumination-acquisition blocks.

without acquiring any interference pattern. The second step consists of monitored thermal homogenisation over a predefined period, after which the temperature gradient is applied. This initiates the third stage, known as the Soret separation phase. Within the Soret phase, three distinct steps are defined: Soret 1, Soret 2, and Soret 3 to track the separation between species as the mixture progresses toward a steady-state plateau. For further details on the Soret cell assembly, optical installation and followed experimental procedure please refer to the following works [28,33].

3. Methodology and results

After each thermodiffusion experiment, image processing is performed to obtain the concentration variations of the mixture's components based on the captured interferograms. The DCMIX missions have outlined a roadmap with various methods to follow the necessary steps for the final determination of the mass transport coefficients of the delivered systems [34]. In previous campaigns, two sets of data could be analysed, since, after the temperature difference was applied for a certain period, the sample was re-homogenised by eliminating the.

Gradient and returning to the average working temperature (referred to as the Diffusion step). However, in the current DCMIX4 mission, the Diffusion step was omitted, leaving only the Soret step for analysis. In this manner, Fig. 2 illustrates the processing pipeline adopted in this work, with the subsequent sections providing a detailed description of each stage in the workflow along with the obtained results: Data Obtention (1), Data Quality Assessment (2), Phase & Refractive Index Maps (3), Data Fitting to Analytical Equation (4), Mass Transport Coefficients (5) and Microgravity vs. Ground Results Comparison (6).

3.1. Data Obtention

The first step involved compiling a database containing the images from each thermodiffusion experiment performed in the 6-reference cell. At present, the database is publicly accessible via the Human and Robotic Exploration Data Archive (HREDA) portal [35]. This platform hosts research data funded by the European Space Agency (ESA) and provides access to data related to all the experiments conducted during the various DCMIX campaigns. All image data are stored in Flexible Image Transport System (FITS) format. For DCMIX4, the companion cell data is organised together with the interferograms from cell 5 (run names: 5r01, 5r02, 5r02r, 5r03, and 5r04), with a total of fifteen images stored in each file. Within every data stack, the first ten consecutive images correspond to the ternary Ps|Tol|Ch mixture (captured using the MN and MR lasers), while the last five images, i.e. the ones assessed during this work, correspond to the binary Ps|Tol subsystem collected using the FR laser. For each run, two additional Excel files are available, containing information on driving current, temperatures of the three laser diodes, and temperatures of the top and bottom layers of the Soret cell. In DCMIX4 four different working temperatures were investigated and, in this work, each thermodiffusion experiment performed in the companion cell is labelled as follows: 6r01 (20 °C), 6r02 and 6r02r (25 °C, two repetitions), 6r03 (30 °C), and 6r04 (35 °C).

3.2. Data quality assessment

Prior to extracting the 2D-Phase maps from the interference patterns, it was essential to individually assess their quality. Within this framework, Mialdun et al. [28] recently reported an analysis of the Data Quality Assessment for the DCMIX4 experiments. Therefore, in this work, the same procedure outlined in Ref. [28] was considered. A comprehensive description of the approach used is provided in Ref. [28], and the following lines overview the key aspects observed in both [28] and during this work, as they are essential for the subsequent stages of the image processing. The quality of an image was defined by two primary metrics: saturation and contrast, and a histogram served as a

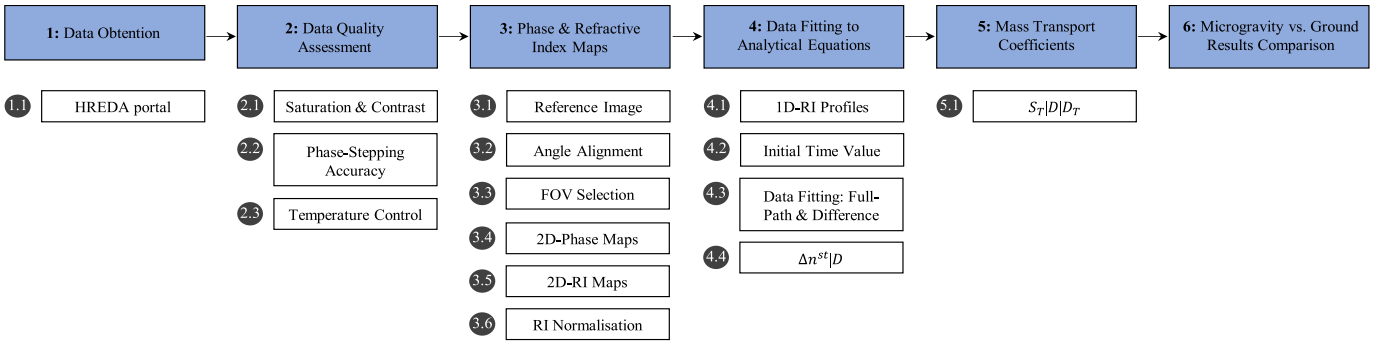

Fig. 2. This work used a sequential process, starting with the establishment of a database and resulting in the determination of the mass transport coefficients of the reference binary polymeric mixture.

crucial tool for determining these parameters. In the case of saturation, an excessive number of saturated pixels in the white (intensity value of 255) or black (intensity value of 0) grey levels can result in a loss of information. As previously reported in Ref. [28], it was observed that all the captured interferograms exceed the minimum white and black saturation thresholds (i.e. less than 5 %) defined by the Experimental Scientific Requirement (ESR) when considering the central region of interest (ROI). Regarding contrast, it was noted that its value is entirely dependent on the method used for its calculation. In this work, the first two approaches presented in Ref. [28] were considered. The first method (and defined via the ESR) describes the contrast as $(I_{max} - I_{min})/(I_{max} + I_{min})$ where I_{max} and I_{min} are the maximum and minimum intensity levels in the selected ROI. However, in general, this equation overestimates the contrast values because if the minimum grey level found in the analysed region is equal to $I_{min} = 0.0$ (even if it is only a single pixel), the approach yields a maximum contrast magnitude. Therefore, as detailed in Ref. [28], an improved second method was considered, limiting the grey levels as follows: I_{min} refers to the average of the lowest 20 % of pixels in terms of grey level, and I_{max} represents the average of the highest 20 % of pixels in terms of grey level. Thus, an experiment was considered disturbed when the number of affected interferograms exceeded 50 % of the total number of images [28]. In this context, this issue was not observed in the thermodiffusion experiments corresponding to the companion cell, at least when applying the described contrast calculation methods.

As mentioned above, SODI is based on the phase-stepping method during the image acquisition process. For this reason, Phase-Stepping Accuracy evaluation was fundamental to ensure the later correct reconstruction of the 2D-Phase shift maps ($\phi(x,z)$). A modified Hariharan algorithm Eq. (1) [36] was used to obtain the phase shift $\phi(x,z)$ from the two-dimensional intensity (I_i) of the five phase-shifted interferograms, as it was successfully employed in previous DCMIX missions [37]. As a consequence of the used arc-tangent in Eq. (1), the obtained phase was mathematically wrapped to the interval -π to +π, and subsequently, a so-called phase unwrapping procedure had to be employed. In this work, the unwrapped phase shift was acquired by the growing pixels method described via Itoh's algorithm [38]. As in the work [28], the error on the phase calculation was defined as the standard deviation between the unwrapped phase (determined) and its linear interpolation. Then, this magnitude was formulated as a percentage of the standard deviation of a three-phase ratio of the full signal (refer to Ref. [28] for a detailed description). Thus, and as previously outlined in Ref. [28], it was observed that experiments 6r02r and 6r04 were the most affected ones. This issue later became apparent when extracting the phase shift variation ($\Delta\phi_z$) as a function of time, by calculating the phase shift difference between two points (top and bottom) of the selected ROI. For this reason, erroneous experimental data points, randomly distributed in time, were observed (refer to Fig. 4).

$$\phi(x,z) = \arctan\left[\frac{7(I_4 - I_2)}{4I_1 - I_2 - 6I_3 - I_4 + 4I_5}\right] \quad (1)$$

Just as image quality and the accuracy of the phase-stepping method are essential, temperature control is a critical aspect in thermodiffusion experiments, since thermodiffusion processes directly depend on the applied temperature gradient. From the recorded temperature data, and following the methods proposed in Ref. [28], the average working temperatures (T_0), the applied temperature gradients (ΔT), and their standard deviations (σ_{T_0} and $\sigma_{\Delta T}$) were calculated together with the presence of spikes that may completely corrupt the data. Additionally, the temperature gradient build-up time (t_{grad}) was determined [28] which is a crucial parameter in order to know when the temperature gradient is fully established. As also mentioned in Ref. [28], it was observed that temperature control in the companion cell experiments showed no anomalies remaining stable (both T_0 and ΔT) and without any detection of spikes. Similarly, in all experiments, it was noted that the t_{grad} times were relatively short, ranging from 117 to 149 s (see Table 1), thus enabling the acquisition of more accurate results when reconstructing the 2D-phase shift maps.

3.3. Phase & Refractive Index Maps

Once the data quality evaluation is completed, the third stage of the image processing workflow involves obtaining 2D-Phase maps, from which the two-dimensional refractive index (RI) data is calculated. To this end, the methodology proposed in Ref. [37] was followed, and an overview of the different steps, along with the obtained results, is provided below. As can be seen in Fig. 2 three preliminary steps are required: reference image identification, angle alignment correction, and Field of View (FoV) selection. Firstly, the reference image (Img_{ref}) corresponding to each DCMIX4 companion cell experiment was identified in order to subtract it from each subsequent interferogram and isolate the contribution of the phase change caused by the temperature gradient jump (refer to Fig. 4 to observe this first sharp phase jump after the homogenisation period). Based on the t_{grad} values presented in Table 1, Img_{ref} was selected as the image captured after the sensors had established the temperature difference over the

Mixture. In all cases, additional time was allowed in order to ensure

Table 1
This work used t_{grad} values [28] along with the selected Img_{ref} and calculated t_0 periods for each thermodiffusion experiment.

$Experiment_{ID}$	t_{grad} (s) [28]	Img_{ref}	t_0 (s)
6r01	117	165	122
6r02	138	165	142
6r02r	149	168	152
6r03	142	167	142
6r04	134	166	132

Table 2
Solutal contrast factors $(\partial n/\partial c).10^{-2}$ of Ps|Tol 0.02|0.98 mixture at $\lambda = 670.0$ nm and as a function of temperature.

Temperature (°C)	$(\partial n/\partial c)$ $\lambda = 670.0$ nm
20	8.95
25	9.03
30	9.10
35	9.18

an optimal stabilisation of the temperature gradient. The following Fig. 3 (a) shows, as an example, the process followed for the selection of the Img_{ref} (experiment 6r01). Table 1 presents the selected reference image for each thermodiffusion experiment. Secondly, the alignment between the companion cell and the CCD camera was checked and adjusted by rotating the captured images 0.08° counterclockwise around their central point. As a last step, interferograms were cropped from 1920 × 1080 pixels to 1530 × 765 pixels, corresponding to a FOV of 10 × 5 mm. Thus, only the central ROI related to the fluid zone was defined, excluding areas associated with the sidewalls and copper plates. In this context, Fig. 3 (b and c) illustrates the selected ROI, along with the corresponding verification for experiment 6r01. The verification of the defined region of interest was done by placing a vertical line at the image center and comparing intensity results from the full frame and the selected ROI.

After the previous preparatory steps were completed, a modified Hariharan algorithm Eq. (1) [36] was used in order to obtain the 2D-Phase maps together with the Itoh's algorithm for its unwrapping [38]. An initial phase shift difference $\Delta\phi_z$ analysis (see Fig. 4) was performed tracking the phase difference between the top and bottom of the complete Soret cell. As the Img_{ref} either the first interferogram captured during the homogenisation period or the reference images previously selected and presented in Table 1 were used. This study enabled the verification of the proper execution of the companion cell DCMIX4 thermodiffusion experiments together with the detection of any anomaly. Furthermore, experiments conducted under the same temperature conditions (6r02 and 6r02r) were compared. In Fig. 4, it is observed that in all conducted experiments $\Delta\phi_z$ remains basically constant during the homogenisation period. Following this, due to the application of the temperature difference, a first sharp phase jump is noted. Once ΔT is established, species separation begins due to diffusion processes, and after a certain period of time the phase difference reaches a steady-state plateau. In the case of the experiments 6r02r and 6r04, erroneous experimental data points were found at different time instants. This is consistent with our analysis of image quality in Ref. [28]. In these runs, more than 25 % of the stacks were deemed insufficient for applying the phase-shifting method for phase extraction, with run 6r02r being the most affected. Both runs were conducted at the end of the mission. The issues are attributable to laser instabilities, which led to the incorrect phase-shifting of one of the images in the stack. However, the runs remain useable. By manually removing the erroneous points, it is still possible to estimate the magnitude of the phase difference, as well as the diffusion coefficient, by fitting the profile as a function of time. For this reason, as it is shown in Fig. 4, once ΔT is established, wrong data points in experiments 6r02r and 6r04 were excluded for further analysis. Thus, in all thermodiffusion experiments (see Fig. 4), the magnitude of the phase difference in the steady-state regime is clearly observed. Similarly, this value varies slightly as a function of the operating temperature, noting that the steady-state phase separation decreases as the system working temperature increases. In addition, it is perceived that the experiments 6r02 and 6r02r, conducted at the same working temperature, show good repeatability. All these observations are further studied quantitatively through the analytical data fittings performed to determine the mass transport coefficients (refer to Table 3).

After extracting the 2D-Phase maps and carrying out the necessary phase variation analysis, Eq. (2) was used in order to calculate the time based 2D-RI maps $(n(x,z))$ [37]. In Eq. (2), λ corresponds to the laser wavelength ($\lambda = 670.0$ nm) and L refers to the path of the laser beam through the liquid volume along the Soret cell ($L = 10.0$ mm). In this context, the extracted phase, and as a result, the derived refractive index was subjected to ambiguity in its absolute value. Thus, normalisation of the refractive index was performed. Similar to the approach proposed in Ref. [37], the refractive index value averaged over the selected ROI was subtracted $n'(x,z) = n(x,z) - \langle n(x,z)\rangle_{ROI}$.

$$n(x,z) = \frac{\lambda}{2\pi L}\phi(x,z) \tag{2}$$

3.4. Data fitting to analytical equations

Once the 2D-Phase and the 2D-RI maps were calculated, the fourth stage of the pipeline involved using different analytical equations in order to fit the experimental data and extract the required parameters to determine the mass transport coefficients of the binary polymeric mixture under analysis. In this context, a prior step was to convert the obtained 2D-RI maps into 1D-RI profiles. Considering [37], the previously normalised RI maps were averaged in the horizontal direction within a selected vertical band of pixels from the map. This is done to ignore the central area of the Soret cell where the channel to the compensation volume is located. Likewise, the influence of the cell corners with non-linear temperature on the resulting profile is prevented (refer to Ref. [37] for more details). Even so, and as previously outlined in Ref. [37], the calculated 1D-RI profiles did not present the expected perfectly linear shape in the steady-state plateau and particular deviations were observed at the boundaries. This is due to the fact that by subtracting the Img_{ref} (selected once the temperature gradient is established) information regarding the species separation at time t_{grad} is lost [37]. Therefore, Mialdun et al. [37] suggested a correction to account for this loss in separation by incorporating an initial time value (t_0) into the fitting algorithm. Thus, in this work, the same approach was considered. The correction involves identifying a time interval starting from the hypothetical stepwise application of the temperature difference up to the selected reference image. In this manner, the concentration profile analytically calculated for this time t_0 is then added to all

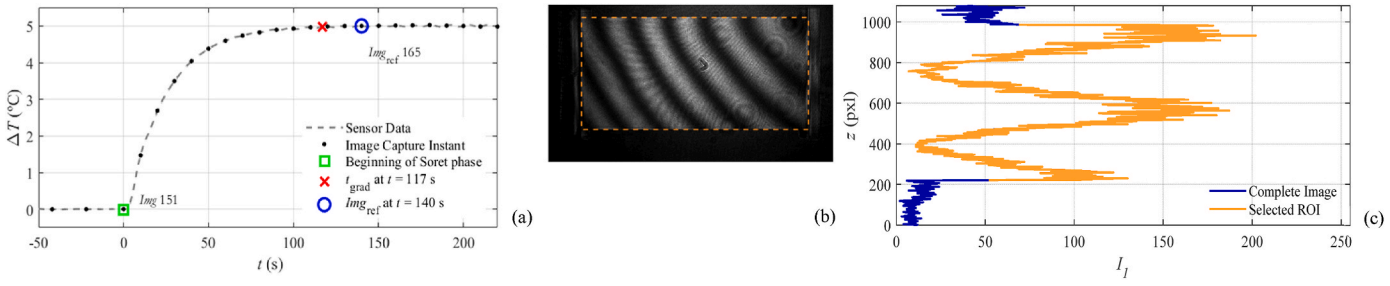

Fig. 3. Preliminary steps followed before extracting the 2D-Phase maps: (a) reference image selection based on recorded temperature data, along with the calculated t_{grad} value; (b) alignment angle correction and central FoV selection; and (c) verification of the defined region of interest. Results correspond to experiment 6r01.

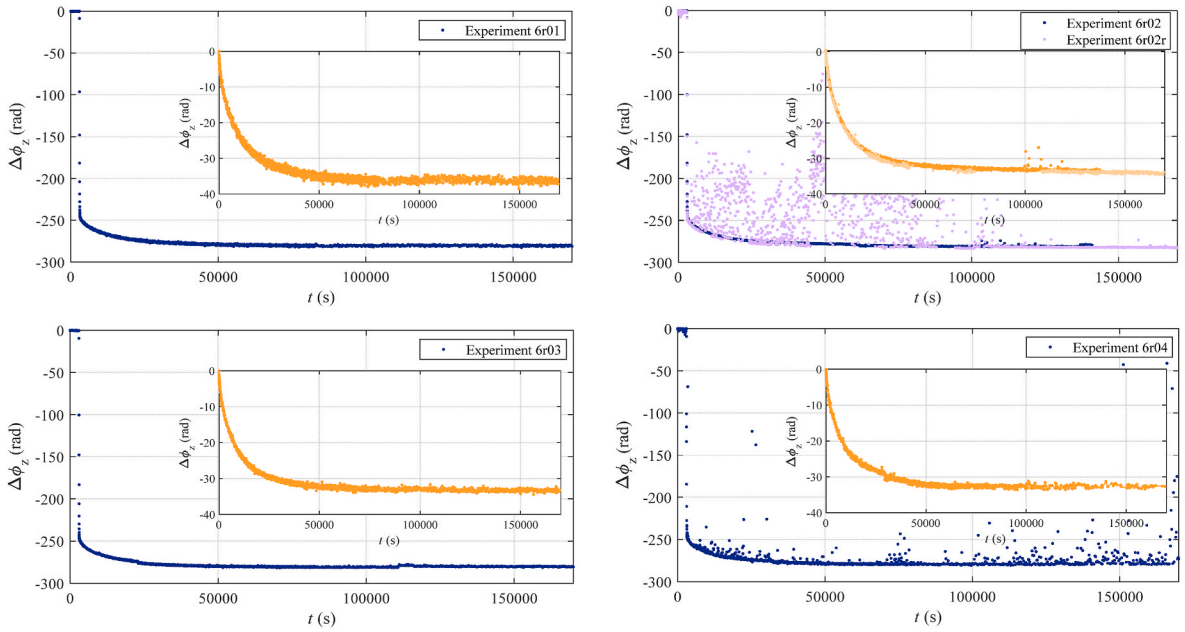

Fig. 4. This work determined $\Delta\phi_z$ as a function of time via considering the total height of the cell and two different reference image instants: experiments 6r01, 6r02 and 6r02r, 6r03 and 6r04. In each case, the large graph corresponds to the data from the complete test, and the insert to the data (same experiment) after the stabilisation of the temperature difference.

Table 3
DCMIX4 companion cell microgravity experiments results. This work determined $\Delta n_z^{st}.10^{-4}$ and $D.10^{-10}$ values using different analytical equations together with the calculated $S_T.10^{-2}$ and $D_T.10^{-12}$ coefficients.

Experiment$_{ID}$	Method	Δn_z^{st}	S_T (1/K)	D (m^2/s)	D_T (m^2/sK)
6r01	Full-Path	−3.93	4.48	2.07	9.28
	Difference	−3.96	4.64	2.20	10.2
	Slopes	−4.18	4.76	1.84	8.74
6r02	Full-Path	−3.71	4.19	2.22	9.32
	Difference	−3.69	4.28	2.32	9.93
	Slopes	−3.97	4.48	1.97	8.81
6r02r	Full-Path	−3.81	4.30	2.11	9.08
	Difference	−3.79	4.40	2.14	9.41
	Slopes	−4.07	4.59	1.88	8.62
6r03	Full-Path	−3.67	4.11	2.36	9.70
	Difference	−3.72	4.28	2.55	10.9
	Slopes	−3.92	4.40	2.15	9.44
6r04	Full-Path	−3.48	3.87	2.57	9.92
	Difference	−3.46	3.95	2.66	10.5
	Slopes	−3.73	4.14	2.27	9.41

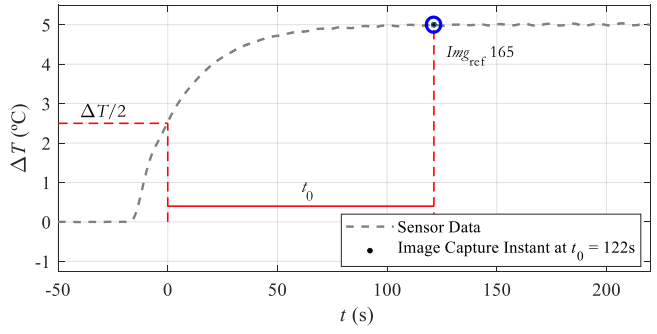

Fig. 5. Schematic illustration of initial the time t_0 determination for the 6r01 experiment.

experimental profiles. A key aspect of this method is the proper selection of the reference time as it is assigned a value of zero and serves as the starting point for calculating the concentration separation. In this work, this time was defined as the period when $\Delta T(t) = \langle \Delta T \rangle / 2$. Fig. 5 shows a representative scheme of the time t_0 for the experiment 6r01 and Table 1 reports the obtained t_0 values for the remaining experiments.

Since a binary system is being studied, two different two-parameter fitting approaches, both previously validated, were employed in order to determine the molecular diffusion coefficient of the mixture (unsteady-state analysis) and the steady-state RI variation (Δn_z^{st}) along with the corresponding concentration separation (Δc_z^{st}). On the one hand, the Full-Path solution was considered Eq. (3) making use of all the available RI data points in both z-space and time ($n(z,t)$) [37]. On the other hand, the Difference method was employed Eq. (4). Temporal differences in refractive index ($\Delta n_z(t)$) between two points of the Soret cell were determined, giving more weight to data points near the two layers. At this point, 10 pixels were excluded from each side of the cell in order to prevent the corner effects (thus 1530 × 745 pixels corresponding to a FOV of 10 × 4.87 mm). This analytical equation is the same as the one used for the data analysis in the μTGC [39]. Additionally, a variation of this approach, called in this work as the Slopes method, was considered. Thus, $\Delta n_z(t)$ was calculated by a first order polynomial fitting of the 1D-RI profiles over the entire cavity. In both methods Eq. (3) and Eq. (4), H corresponds to the height of the cell ($H = 5.0$ mm) and t to the time. A geometrical parameter, $a = \frac{4H}{\Delta H}\left(\cos\left(\frac{\pi H_1}{H}\right) - \cos\left(\frac{\pi H_2}{H}\right)\right)$, appears in Eq. (4), which depends on the two boundaries (H_1 and H_2) where RI difference is calculated.

$$n'(z,t) = \Delta n_z^{st}\left[-\frac{1}{2} + \frac{z}{H} + \frac{4}{\pi^2}\sum_{k,odd}^{\infty}\frac{1}{k^2}\cos\left(\frac{k\pi z}{H}\right)e^{\left(-\frac{k^2\pi^2}{H^2}Dt\right)}\right] \tag{3}$$

$$\frac{\Delta n_z(t)}{\Delta n_z^{st}} = 1 - \frac{a}{\pi^2}\sum_{k,odd}^{\infty}\frac{1}{k^2}e^{\left(-\frac{k^2\pi^2}{H^2}Dt\right)} \tag{4}$$

The following Fig. 6 presents, as an example, the obtained results

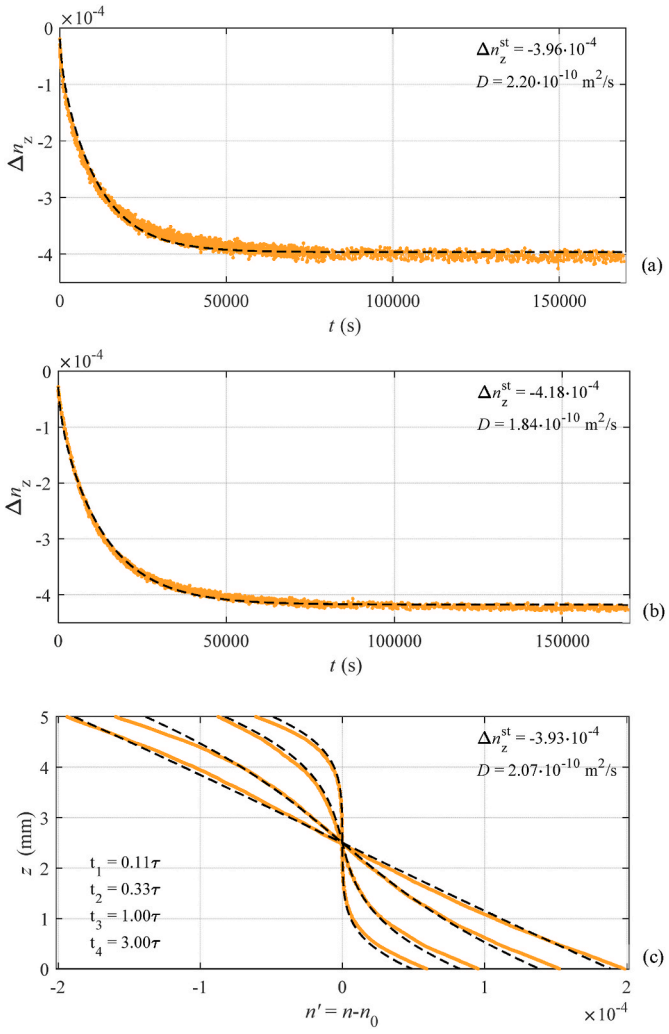

Fig. 6. Fitting of 1D-RI profiles of DCMIX4 companion cell Ps|Tol 0.02|0.98 binary mixture (experiment 6r01 performed at $T_0 = 20$ °C) via different analytical solutions and considering $t_0 = 122$ (s): (a) Difference method, (b) Slopes approach and (c) Full-Path algorithm being $\tau = H^2/(\pi^2 D)$.

from fitting the 1D-RI Profiles of experiment 6r01 via considering the different analytical equations mentioned above. As a first qualitative observation, it can be noted that the three approaches provide a good fit for the experimental data. Even so, regarding the quantitative analysis of the determined Δn_z^{st} (steady-state regime data points) and D (transitory data points) values, it can be observed that Δn_z^{st} magnitudes (calculated by the distinct algorithms) are closer to each other than the extracted molecular diffusion coefficients. This could be because transient data analysis is generally less stable and tends to exhibit larger deviations. Similarly, it is found that via the slopes method, and in comparison with D magnitudes reported in Ref. [30], a lower diffusion coefficient is obtained. The fitting parameters extracted for each experiment are presented in Table 3 along with their subsequent analysis in the following section 3.5.

3.5. Mass transport coefficients

The fifth stage of the workflow consisted in determining the mass transport coefficients of the polymeric subsystem Ps|Tol 0.02|0.98 at different operating temperatures once Δn_z^{st} and D were previously extracted via different analytical methods. In the case of the Soret coefficient, first, Δn_z^{st} was converted into Δc_z^{st} by means of the solutal contrast factors ($\partial n/\partial c$) determined for each working temperature and an operating wavelength of $\lambda = 670.0$ nm (corresponding to FR laser) $\Delta n_z^{st} = (\partial n/\partial c)\Delta c_z^{st}$. This work employed solutal contrast factors, as shown in Table 2, determined using the methodology based on Cauchy's dispersion equation, as previously described in Ref. [30]. Thus, it was possible to calculate the Soret coefficient of the binary polymeric mixture using Eq. (5) where c_0 refers to the initial concentration of the densest component of the system. At the same time, the indirect calculation of the thermodiffusion coefficient was performed being $D_T = S_T D$. Both S_T and D_T are presented in the following Table 3.

$$S_T = -\frac{1}{c_0(1-c_0)}\frac{\Delta c_z^{st}}{\Delta T} \tag{5}$$

Regarding the results presented in Table 3, on the one hand, in relation to the steady-state analysis, it can be noted that the fitted Δn_z^{st} values (independent of the used algorithm) present a decreasing trend as a function of the working temperature. This is later reflected in the calculation of the Soret coefficient, which also shows a linear decreasing tendency as the temperature increases (see Fig. 7). At the same time, it can be observed that S_T magnitudes differ slightly (maximum deviation of 7 % in the experiment 6r03) depending on the used analytical equation. In all cases, the Soret coefficients obtained by means of the Slopes method are the largest. This, in comparison with the difference method, could be due to the fact that instead of studying only the RI difference between two points in the cell, the species separation along the entire cavity is considered. As for the experiments 6r02 and 6r02r conducted at the same working temperature, it can be observed that the first experiment exhibits a lower Soret coefficient. In this context, the

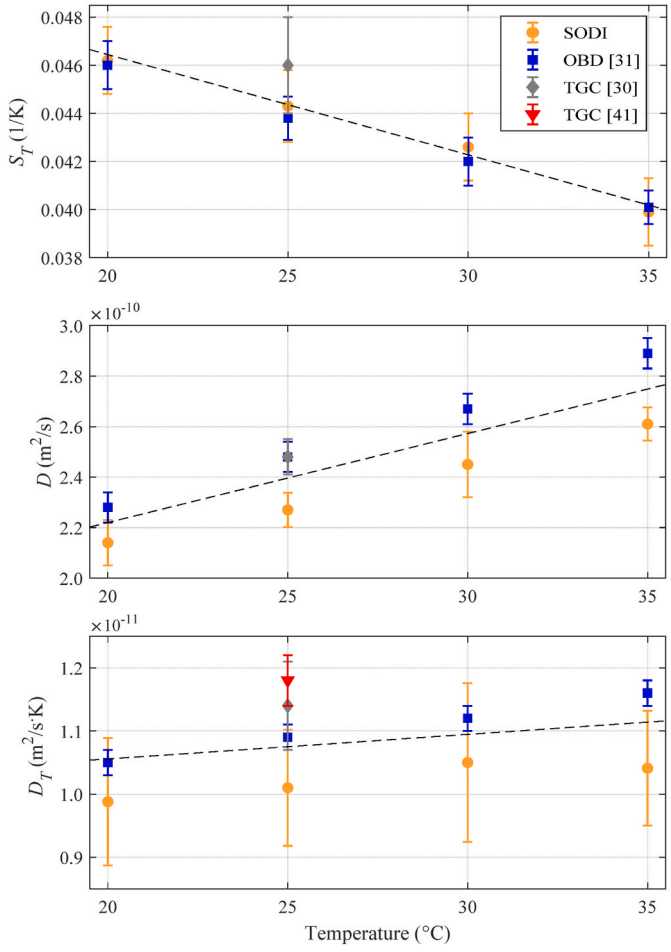

Fig. 7. Ps|Tol 0.02|0.98 mixture Soret, molecular diffusion and thermodiffusion coefficients as a function of temperature. Comparison between microgravity (DCMIX4 campaign) and gravity-based results.

reason for this could be that the steady-state separation was not fully reached, as the 6r02 experiment duration was shorter (see Fig. 4).

On the other hand, regarding the transient data analysis, it can be observed that the calculated diffusion coefficients present an increasing tendency as the temperature rises. In all cases, D coefficients obtained by the Full-Path and the Difference methods are closer to each other than the ones extracted via the Slopes approach. In this manner, it seems that the steady-state species separation is reached earlier by calculating $\Delta n_z(t)$ through a first-order polynomial fit of the 1D-RI profiles across the entire cell. For this reason, the extracted diffusion coefficients using the Slopes method exhibit a lower magnitude. In addition, regarding the experiments 6r02r and 6r04 (see Fig. 4), it can be observed that the obtained D coefficients are affected by the phase-stepping method quality (see Fig. 4) resulting in lower diffusion magnitudes as well. Subsequently, as for the obtained D_T coefficients, it is noted that the thermodiffusion coefficient presents an increasing tendency as the operating temperature increases. Nevertheless, a larger uncertainty is observed as the thermodiffusion coefficient is calculated indirectly and is completely dependent on the previously determined S_T and D.

3.6. Microgravity vs. Ground Results Comparison

The last step of the pipeline consisted of comparing the obtained mass transport coefficients (microgravity environment) with gravity-based results (see Fig. 7). Under ground conditions, thermodiffusion experiments were conducted using two different experimental methods, both in convective and non-convective regimes. The traditional TGC technique (MGEP, Spain) together with the OBD method (UB, Germany) were considered. Additionally, data from bibliography based on the TDFRS technique was included for comparison [40]. Gravity-based results were previously published in the following works [30,31]. As for microgravity results, data from Table 3 was considered. On the one hand, regarding the Soret coefficient, for each working temperature, the average of the different S_T values extracted through the various analytical equations was calculated. Data from experiment 6r02 was excluded since the temperature gradient period was not long enough to achieve the steady-state plateau. On the other hand, diffusion coefficient was determined considering the average between the D magnitudes acquired by the Full-Path and the Difference Methods. Molecular diffusion coefficient from experiment 6r02r was not considered due to the poor quality of the phase-stepping method. As a result, D_T was indirectly calculated. Table 4 summarises the transport coefficients determined from microgravity experiments together with the obtained deviations considering the different analytical solutions and Fig. 7 presents a first comparison between ground and microgravity results.

4. Conclusions

In this work, we have presented a detailed evaluation of the results of the DCMIX4 thermodiffusion experiments carried out on board the ISS. The analysis focuses on a companion cell filled with a binary mixture of polystyrene dissolved in pure toluene (Ps molar mass 4730 g/mol and 0.02|0.98 mass fraction). After full data processing, the Soret and diffusion coefficients of the macromolecular mixture were obtained together with the indirect calculation of the thermodiffusion coefficients. Mass transport coefficients were extracted at the working temperatures of 20–25-30-35 °C. Although we were investigating binary mixtures, the excellent agreement between the microgravity and ground-based results demonstrates the tremendous progress made in processing raw data from the ISS since the DCMIX1 campaign, when the benchmark results [17] showed larger deviations. Additionally, this study will be essential for initiating the investigation of the ternary macromolecular mixture under microgravity conditions.

Table 4
Ps|Tol 0.02|0.98 mixture mass transport coefficients $S_T.10^{-2}$, $D.10^{-10}$ and $D_T.10^{-12}$ determined from DCMIX4 microgravity experiments.

Temperature (°C)	S_T (1/K)	D (m^2/s)	D_T (m^2/sK)
20	4.62 ± 0.14	2.14 ± 0.09	9.88 ± 1.0
25	4.43 ± 0.15	2.27 ± 0.07	10.1 ± 0.8
30	4.26 ± 0.14	2.45 ± 0.13	10.4 ± 1.3
35	3.99 ± 0.14	2.61 ± 0.07	10.4 ± 0.9

CRediT authorship contribution statement

Antton Sanjuan: Data curation, Formal analysis, Investigation, Methodology, Writing – original draft, Writing – review & editing, Validation, Visualization. **Daniel Sommermann:** Data curation, Formal analysis, Investigation, Methodology. **Werner Köhler:** Conceptualization, Data curation, Funding acquisition, Project administration, Resources, Supervision, Validation, Visualization, Writing – review & editing. **Henri Bataller:** Conceptualization, Data curation, Formal analysis, Funding acquisition, Project administration, Resources, Validation, Writing – review & editing. **Fabrizio Croccolo:** Conceptualization, Data curation, Formal analysis, Funding acquisition, Project administration, Resources, Validation, Writing – review & editing. **Aliaksandr Mialdun:** Conceptualization, Data curation, Formal analysis, Investigation, Methodology, Validation, Writing – review & editing. **Valentina Shevtsova:** Conceptualization, Data curation, Funding acquisition, Project administration, Resources, Validation, Visualization, Writing – review & editing. **M. Mounir Bou-Ali:** Conceptualization, Data curation, Funding acquisition, Project administration, Resources, Supervision, Validation, Visualization, Writing – review & editing.

Declaration of competing interest

The authors declare that they have no known competing financial interests or personal relationships that could have appeared to influence the work reported in this paper.

Acknowledgements

A.S. would like to thank the Basque Government for funding through an FPI grant (PRE_2024_2_0226). M.M.B., V.S., and A.M. would like to acknowledge financial support from the Basque Government SMARTμS project (KK-2025/00058) and the Research Group Programme (IT1505-22) and the Spanish Government projects PID2023-149539NB-C33 (MICINN/FEDER), and PCI2024-155071-2 (MCINN/AEI). D.S. and W.K. acknowledge support by Deutsches Zentrum für Luft-und Raumfahrt (DLR, Grants No. 50WM2147, 50WM2444) and by Deutsche Forschungsgemeinschaft (DFG, Grant No. DFG, KO1541/13-1). F.C. and H.B. acknowledge partial support under the framework of the E2S-UPPA Hub Newpores and Industrial Chair CO2ES, supported by the Investissements d'Avenir French Program managed by ANR (No. ANR161-DEX0002). F.C. and H.B. also acknowledge partial support from the CNES through the GdR 2799 MFA.

References

[1] C. Ludwig, "Diffusion zwischen ungleich erwärmten Orten gleich zusammengesetzter Lösungen," Sitz. Ber. Akad. Wiss. Wien Math-Naturw, vol. 20, p. 539, 1856.
[2] W. Köhler, K.I. Morozov, The soret effect in liquid mixtures – a review, J. Non-Equilibrium Thermodyn. 41 (3) (Jan. 2016), https://doi.org/10.1515/jnet-2016-0024.
[3] W. Köhler, A. Mialdun, M.M. Bou-Ali, V. Shevtsova, The measurement of soret and thermodiffusion coefficients in binary and ternary liquid mixtures, Int. J. Thermophys. 44 (9) (Sep. 2023) 140, https://doi.org/10.1007/s10765-023-03242-x.
[4] M.M. Bou-Ali, J.J. Valencia, J.A. Madariaga, C. Santamaría, O. Ecenarro, J. F. Dutrieux, Determination of the thermodiffusion coefficient in three binary

organic liquid mixtures by the thermogravitational method (contribution of the Universidad del País Vasco, Bilbao, to the benchmark test), Philos. Mag. 83 (17–18) (Jan. 2003) 2011–2015, https://doi.org/10.1080/0141861031000113299.
[5] G. Wittko, W. Köhler, Precise determination of the soret, thermal diffusion and mass diffusion coefficients of binary mixtures of dodecane, isobutylbenzene and 1,2,3,4-tetrahydronaphthalene by a holographic grating technique, Philos. Mag. 83 (17–18) (Jan. 2003) 1973–1987, https://doi.org/10.1080/01418610310001082l3.
[6] J.K. Platten, M.M. Bou-Ali, J.F. Dutrieux, Precise determination of the soret, thermodiffusion and isothermal diffusion coefficients of binary mixtures of dodecane, isobutylbenzene and 1,2,3,4-tetrahydronaphthalene (contribution of the university of Mons to the benchmark test), Philos. Mag. 83 (17–18) (Jan. 2003) 2001–2010, https://doi.org/10.1080/01418610310001081.96.
[7] J.K. Platten, M.M. Bou-Ali, P. Costesèque, J.F. Dutrieux, W. Köhler, C. Leppla, S. Wiegand, G. Wittko, Benchmark values for the Soret, thermal diffusion and diffusion coefficients of three binary organic liquid mixtures, Philos. Mag. 83 (17–18) (Jan. 2003) 1965–1971, https://doi.org/10.1080/01418610310001082.04.
[8] A. Königer, B. Meier, W. Köhler, Measurement of the Soret, diffusion, and thermal diffusion coefficients of three binary organic benchmark mixtures and of ethanol–water mixtures using a beam deflection technique, Philos. Mag. 89 (10) (Apr. 2009) 907–923, https://doi.org/10.1080/14786430902814029.
[9] A. Mialdun, V. Shevtsova, Measurement of the Soret and diffusion coefficients for benchmark binary mixtures by means of digital interferometry, J. Chem. Phys. 134 (4) (Jan. 2011), https://doi.org/10.1063/1.3546036.
[10] E. Lapeira, A. Mialdun, V. Yasnou, P. Aristimuño, V. Shevtsova, M.M. Bou-Ali, Digital interferometry applied to thermogravitational technique, Microgravity Sci. Technol. 30 (5) (Oct. 2018) 635–641, https://doi.org/10.1007/s12217-018-9632-7.
[11] F. Croccolo, H. Bataller, F. Scheffold, A light scattering study of non equilibrium fluctuations in liquid mixtures to measure the Soret and mass diffusion coefficient, J. Chem. Phys. 137 (23) (Dec. 2012), https://doi.org/10.1063/1.4771872.
[12] M.M. Bou-Ali, J.K. Platten, Metrology of the thermodiffusion coefficients in a ternary system, J. Non-Equilibrium Thermodyn. 30 (4) (Jan. 2005), https://doi.org/10.1515/JNETDY.2005.027.
[13] P. Blanco, M.M. Bou-Ali, J.K. Platten, D. Alonso de Mezquia, J.A. Madariaga, C. Santamaría, Thermodiffusion coefficients of binary and ternary hydrocarbon mixtures, J. Chem. Phys. 132 (11) (Mar. 2010), https://doi.org/10.1063/1.3354114.
[14] A. Königer, H. Wunderlich, W. Köhler, Measurement of diffusion and thermal diffusion in ternary fluid mixtures using a two-color optical beam deflection technique, J. Chem. Phys. 132 (17) (May 2010), https://doi.org/10.1063/1.3421547.
[15] M. Schraml, T. Triller, D. Sommermann, W. Köhler, The DCMIX project: measurement of thermodiffusion processes in ternary mixtures on ground and in space, Acta Astronaut. 160 (Jul. 2019) 251–257, https://doi.org/10.1016/j.actaastro.2019.04.027.
[16] M. Braibanti, et al., European Space Agency experiments on thermodiffusion of fluid mixtures in space, The European Physical Journal E 42 (7) (Jul. 2019) 86, https://doi.org/10.1140/epje/i2019-11849-0.
[17] V. Shevtsova, W. Köhler, M.M. Bou-Ali, A. Mialdun, Progress in multicomponent thermodiffusion studies in connection with the DCMIX space experiments, Chemical Physics Reviews 5 (3) (Sep. 2024), https://doi.org/10.1063/5.0218425.
[18] M.M. Bou-Ali, A. Ahadi, D. Alonso de Mezquia, Q. Galand, M. Gebhardt, O. Khlybov, W. Köhler, M. Larrañaga, J.C. Legros, T. Lyubimova, A. Mialdun, I. I. Ryzhkov, M.Z. Saghir, V. Shevtsova, S. Van Vaerenbergh, Benchmark values for the Soret, thermodiffusion and molecular diffusion coefficients of the ternary mixture tetralin+isobutylbenzene+n-dodecane with 0.8-0.1-0.1 mass fraction, The European Physical Journal E 38 (4) (Apr. 2015) 30, https://doi.org/10.1140/epje/i2015-15030-7.
[19] A. Mialdun, V. Shevtsova, Temperature dependence of Soret and diffusion coefficients for toluene–cyclohexane mixture measured in convection-free environment, J. Chem. Phys. 143 (22) (Dec. 2015), https://doi.org/10.1063/1.4936778.
[20] E. Lapeira, M. Gebhardt, T. Triller, A. Mialdun, W. Köhler, V. Shevtsova, M.M. Bou-Ali, Transport properties of the binary mixtures of the three organic liquids toluene, methanol, and cyclohexane, J. Chem. Phys. 146 (9) (Mar. 2017), https://doi.org/10.1063/1.4977078.
[21] A. Mialdun, I.I. Ryzhkov, O. Khlybov, T. Lyubimova, V. Shevtsova, Measurement of Soret coefficients in a ternary mixture of toluene–methanol–cyclohexane in convection-free environment, J. Chem. Phys. 148 (4) (Jan. 2018), https://doi.org/10.1063/1.5017716.
[22] P. Kolodner, H. Williams, C. Moe, Optical measurement of the Soret coefficient of ethanol/water solutions, J. Chem. Phys. 88 (10) (May 1988) 6512–6524, https://doi.org/10.1063/1.454436.
[23] E. Lapeira, M.M. Bou-Ali, J.A. Madariaga, C. Santamaría, Thermodiffusion coefficients of Water/Ethanol mixtures for low water mass fractions, Microgravity Sci. Technol. 28 (5) (Oct. 2016) 553–557, https://doi.org/10.1007/s12217-016-9508-7.
[24] M. Schraml, H. Bataller, C. Bauer, M.M. Bou-Ali, F. Croccolo, E. Lapeira, A. Mialdun, P. Möckel, A.T. Ndjaka, V. Shevtsova, W. Köhler, The Soret coefficients of the ternary system water/ethanol/triethylene glycol and its corresponding binary mixtures, The European Physical Journal E 44 (10) (2021) 128, https://doi.org/10.1140/epje/s10189-021-00134-6.
[25] A.T. Ndjaka, L. García-Fernández, D.E.B. Bouyou, A. Lassin, M. Azaroual, F. Croccolo, H. Bataller, Mass diffusion and Soret coefficient measurements of triethylene glycol/water binary mixtures by dynamic shadowgraphy, The European Physical Journal E 45 (3) (Mar. 2022) 20, https://doi.org/10.1140/epje/s10189-022-00171-9.
[26] D. Sommermann, T. Triller, W. Köhler, A Robust data evaluation method for the DCMIX microgravity experiments, Microgravity Sci. Technol. 31 (5) (Oct. 2019) 465–474, https://doi.org/10.1007/s12217-019-09722-w.
[27] T. Triller, D. Sommermann, M. Schraml, F. Sommer, E. Lapeira, M.M. Bou-Ali, W. Köhler, The Soret effect in ternary mixtures of water+ethanol+triethylene glycol of equal mass fractions: ground and microgravity experiments, The European Physical Journal E 42 (3) (2019) 27, https://doi.org/10.1140/epje/i2019-11789-7.
[28] A. Mialdun, et al., Data quality assessment of Diffusion Coefficient Measurements in ternary mIXtures 4 (DCMIX4) experiment, Acta Astronaut. 176 (Nov. 2020) 204–215, https://doi.org/10.1016/j.actaastro.2020.06.020.
[29] A. Errarte, M. Schraml, W. Köhler, V. Shevtsova, M.M. Bou-Ali, A. Mialdun, Thermophysical, optical, and mass transport properties of C 60 fullerene solutions in toluene and Tetralin, J. Chem. Eng. Data 67 (9) (Sep. 2022) 2160–2173, https://doi.org/10.1021/acs.jced.2c00140.
[30] A. Sanjuan, D. Sommermann, W. Köhler, V. Shevtsova, M.M. Bou-Ali, Thermodiffusion, diffusion and Soret coefficients of binary polymeric mixtures in toluene and cyclohexane, J. Non-Equilibrium Thermodyn. 0 (0) (May 2024), https://doi.org/10.1515/jnet-2023-0125.
[31] D. Sommermann, W. Köhler, Diffusion and thermodiffusion of the ternary system polystyrene + toluene + cyclohexane, J. Chem. Phys. 159 (16) (Oct. 2023), https://doi.org/10.1063/5.0176432.
[32] L. García-Fernández, H. Bataller, P. Fruton, C. Giraudet, A. Vailati, F. Croccolo, Stabilized convection in a ternary mixture with two Soret coefficients of opposite sign, The European Physical Journal E 45 (6) (Jun. 2022) 52, https://doi.org/10.1140/epje/s10189-022-00202-5.
[33] A. Mialdun, C. Minetti, Y. Gaponenko, V. Shevtsova, F. Dubois, Analysis of the thermal performance of SODI instrument for DCMIX configuration, Microgravity Sci. Technol. 25 (1) (Feb. 2013) 83–94, https://doi.org/10.1007/s12217-012-9337-2.
[34] Q. Galand, S. Van Vaerenbergh, W. Köhler, O. Khlybov, T. Lyubimova, A. Mialdun, I.I. Ryzhkov, V. Shevtsova, T. Triller, Results of the DCMIX1 experiment on measurement of Soret coefficients in ternary mixtures of hydrocarbons under microgravity conditions on the ISS, J. Chem. Phys. 151 (13) (Oct. 2019), https://doi.org/10.1063/1.5100595.
[35] ESA, HRE data archive. https://hreda.esac.esa.int/hreda/#/pages/home.
[36] P. Hariharan, B.F. Oreb, T. Eiju, Digital phase-shifting interferometry: a simple error-compensating phase calculation algorithm, Appl. Opt. 26 (13) (Jul. 1987) 2504, https://doi.org/10.1364/AO.26.002504.
[37] A. Mialdun, J.-C. Legros, V. Yasnou, V. Sechenyh, V. Shevtsova, Contribution to the benchmark for ternary mixtures: measurement of the Soret, diffusion and thermodiffusion coefficients in the ternary mixture THN/IBB/nC12 with 0.8/0.1/0.1 mass fractions in ground and orbital laboratories, The European Physical Journal E 38 (4) (Apr. 2015) 27, https://doi.org/10.1140/epje/i2015-15027-2.
[38] K. Itoh, Analysis of the phase unwrapping algorithm, Appl. Opt. 21 (14) (Jul. 1982) 2470, https://doi.org/10.1364/AO.21.002470.
[39] B. Šeta, J. Gavalda, M.M. Bou-Ali, X. Ruiz, C. Santamaria, Determining diffusion, thermodiffusion and Soret coefficients by the thermogravitational technique in binary mixtures with optical digital interferometry analysis, Int. J. Heat Mass Tran. 147 (Feb. 2020) 118935, https://doi.org/10.1016/j.ijheatmasstransfer.2019.118935.
[40] J. Rauch, W. Köhler, Collective and thermal diffusion in dilute, semidilute, and concentrated solutions of polystyrene in toluene, J. Chem. Phys. 119 (22) (Dec. 2003) 11977–11988, https://doi.org/10.1063/1.1623745.